ChemCatChem

Supporting Information

Stability of $Pt_{10}Sn_3$ Clusters Supported on γ-Al_2O_3 in Oxidizing Environment: a DFT Comparison of Alloying and Size Effects

Masoud Shahrokhi, Celine Chizallet, David Loffreda, and Pascal Raybaud*

S1. Most stable structure of uncovered $Pt_{10}Sn_3O_n/\gamma\text{-}Al_2O_3$

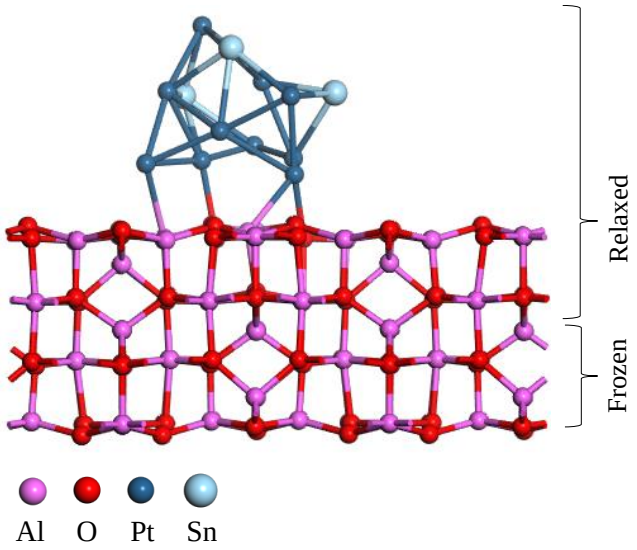

Figure S1. Lateral view of the molecular structure of the starting model of $Pt_{10}Sn_3/\gamma\text{-}Al_2O_3(100)$.

S2. Lattice parameters and corresponding k-point meshes for Pt, Pt_3Sn, PtO, PtO_2, SnO and SnO_2 bulk phases

Bulk phase	Lattice parameters (Å)			k-point mesh
	a	*b*	*c*	
Pt	2.81	2.81	2.81	12 × 12 × 12
Pt_3Sn	4.06	4.06	4.06	10 × 10 × 10
PtO (tetragonal)	3.15	3.15	5.34	10 × 10 × 10
PtO_2 (tetragonal)	4.57	4.57	3.24	10 × 10 × 10
SnO (tetragonal)	3.86	3.86	5.00	10 × 10 × 10
SnO_2 (tetragonal)	4.62	4.62	3.14	10 × 10 × 10

Table S1. Optimized lattice parameters and corresponding k-point meshes for Pt, Pt_3Sn, PtO, PtO_2, SnO and SnO_2 bulk phases.

S3. Illustration of a typical velocity-scaled MD run with cluster reconstruction

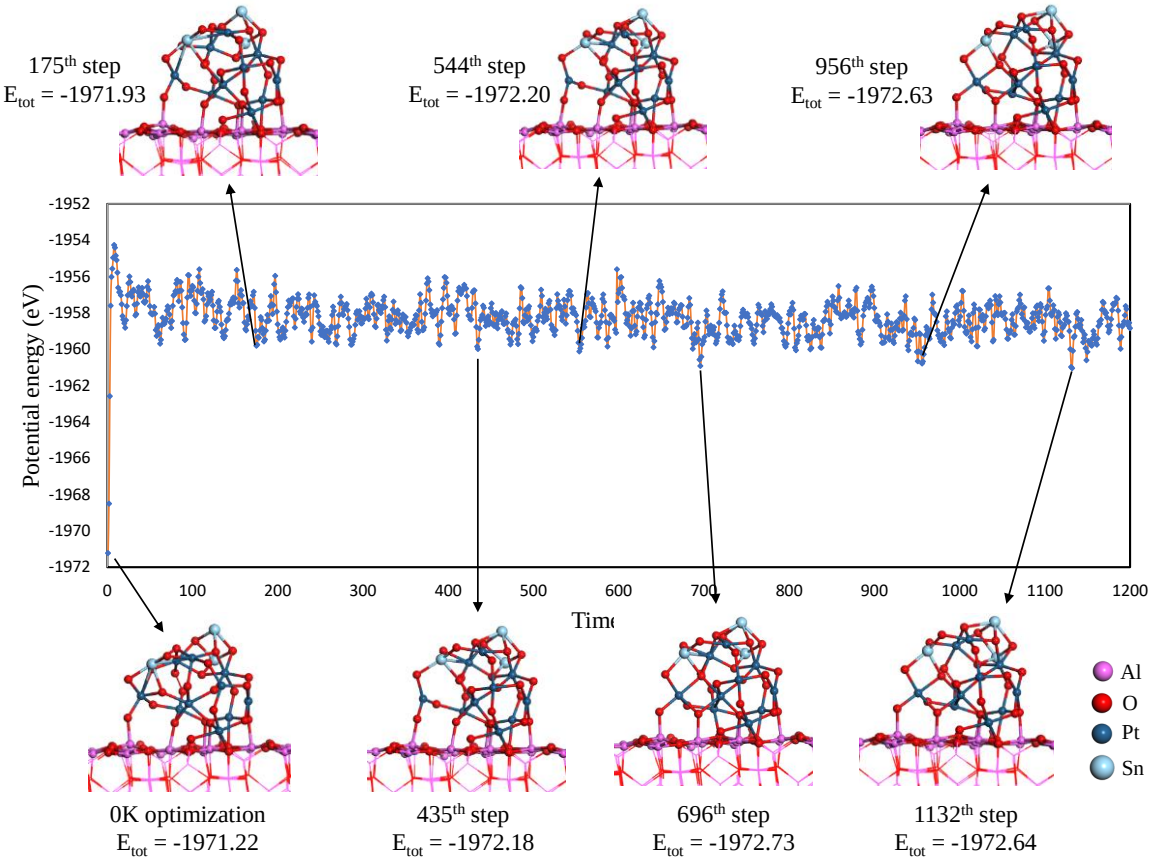

Figure S2. Potential energy *versus* time step for $Pt_{10}Sn_3O_{26}/Al_2O_3$ system through the optimization – velocity-scaled molecular dynamics calculations at 600K and 5fs. For the most stable geometries during the MD run, the obtained structures and total energies by geometry optimization (quench for the final structure) are also presented.

S4. Most stable structures found for the supported $Pt_{10}Sn_3O_n$ system from DFT calculations

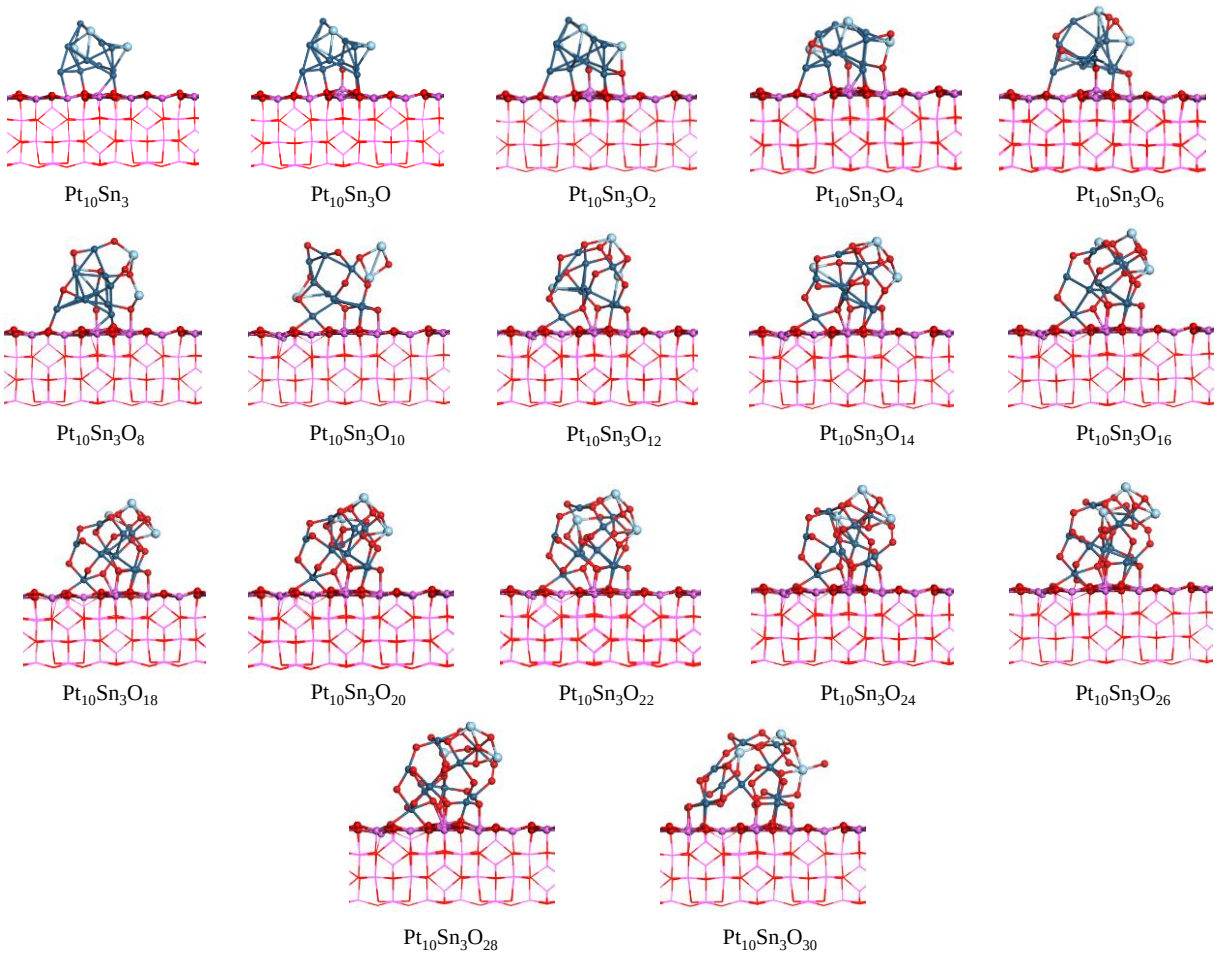

Figure S3**.** Side views of the most stable $Pt_{10}Sn_3O_n/\gamma\text{-}Al_2O_3$ structures. Color code for the atomic structures is the same as in Figure S1.

S5. Estimation of the Gibbs free energy of adsorption

Gibbs free energy was calculated with the following equations

$$G(T,p) = E + U_{trans}(T,p) + U_{vib}(T,p) + U_{rot}(T,p) + PV_m - T\left(S_{trans}(T,p) + S_{vib}(T,p) + S_{rot}(T,p)\right) \quad (Equation\ S1)$$

where E is the electronic energy, S is the entropies, U is thermal energies, p is the pressure and V_m is the molar volume.

$$U_{vib}(T) = N_A\left[\sum_n \frac{1}{2}h\vartheta_n + \sum_n \frac{hc\vartheta_n \times \exp\left(-\frac{h\vartheta_n}{k_BT}\right)}{1-\exp\left(-\frac{h\vartheta_n}{k_BT}\right)}\right] \quad \text{(Equation S2)}$$

Equation S3 is used for the gas specie O_2. In the case of condensed systems ($Pt_{10}Sn_3On/\gamma\text{-}Al_2O_3$), these terms are considered to be zero, as well as rotational and translational entropies given by equations (S5) and (S6).

$$U_{trans}(T) + U_{rot}(T) + PV_m(T) = 7/2\,RT \quad (Equation\ S3)$$

$$S_{vib}(T) = N_A k_B\left[\sum_n \frac{\frac{hc\vartheta_n}{k_BT} \times \exp\left(-\frac{h\vartheta_n}{k_BT}\right)}{1-\exp\left(-\frac{h\vartheta_n}{k_BT}\right)} - \sum_n \ln\left(1-\exp\left(-\frac{h\vartheta_n}{k_BT}\right)\right)\right] \quad (Equation\ S4)$$

$$S_{rot}(T) = N_A k_B\left(\frac{3}{2} + ln\left[\frac{\sqrt{\pi}}{\sigma}\left(\frac{8\pi^2 k_B T}{h^2}\right)^{\frac{3}{2}}\sqrt{A_e B_e C_e}\right]\right) \quad (Equation\ S5)$$

$$S_{trans}(T,p) = N_A k_B\left(\frac{5}{2} + \ln\left(\frac{RT}{p}\left(\frac{2\pi M\ k_B T}{h^2}\right)^{3/2}\right)\right) \quad (Equation\ S6)$$

where k_B is the Boltzmann constant, ν_n is the vibrational frequencies of the system (vibration eigenvalues), N_A is the Avogadro constant, T is the temperature, h is the Planck constant and M the molar weight. σ corresponds to the symmetry number of the system and A_e ,B_e and C_e the moments of inertia according to the eigenaxes of the molecule. The determination of the oxygen-adsorption free energy G used to build the thermodynamic diagrams is detailed in equation 2. The different domains of coverages present on the diagrams reflect the minimum free energy among other coverage systems.

S6. Thermodynamic diagram (P_{O2}, T) for the adsorption of atomic O on Pt(111).

At UHV pressure, the stability of these three distinct phases is as follow: (i) At low temperatures up to ~250 K, the 0.5 ML O ad-atom is the most stable; (ii) over the range between 250 K and 500 K the 0.25ML O ad-atom phase is stable; and (iii) above 500 K the clean Pt (111) surface becomes thermodynamically stable. At no stage any of the higher coverage O ad-atom (0.75 ML and 1 ML) phases become stable. Moreover, on raising the pressure, at a temperature of ~500 K, from UHV to industrial pressures the state of the Pt (111) surface is predicted to change from bare surface to 0.5 ML O ad-atom. Where comparison is possible, our results are in satisfactory agreement with numerous previous DFT studies.[1]

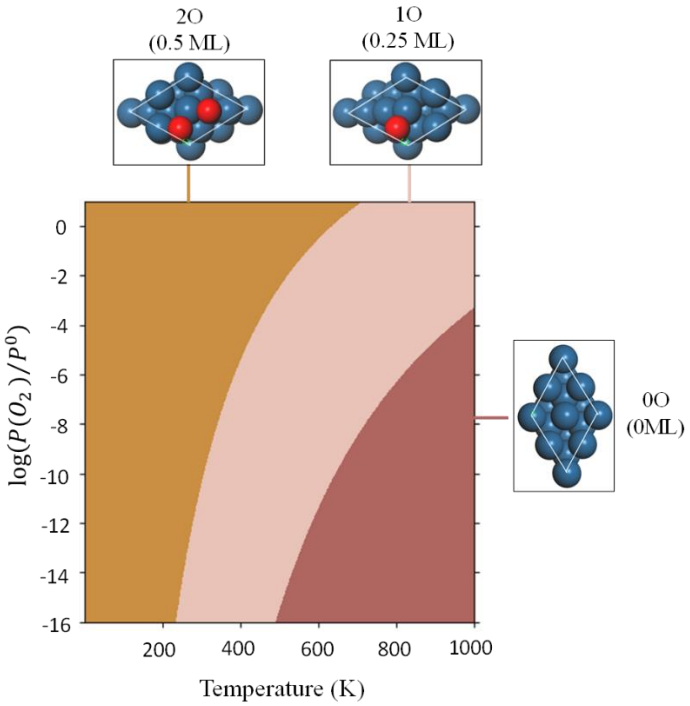

Figure S4. Thermodynamic phase diagram as a function of the temperature (K) and the O_2 partial pressure (bar) depicting for the adsorption of atomic oxygen in fcc sites on Pt (111). The clean Pt (111) surface were modeled by a slab consisting of 5 Pt layer and a 2×2 surface unit cell. The structures of the systems exhibiting a significant stability domain are also depicted (top views). Color code for the atomic structures is the same as in Figure S1.

S7. Most stable structures of oxygen adsorption on Pt_3Sn (111) surface

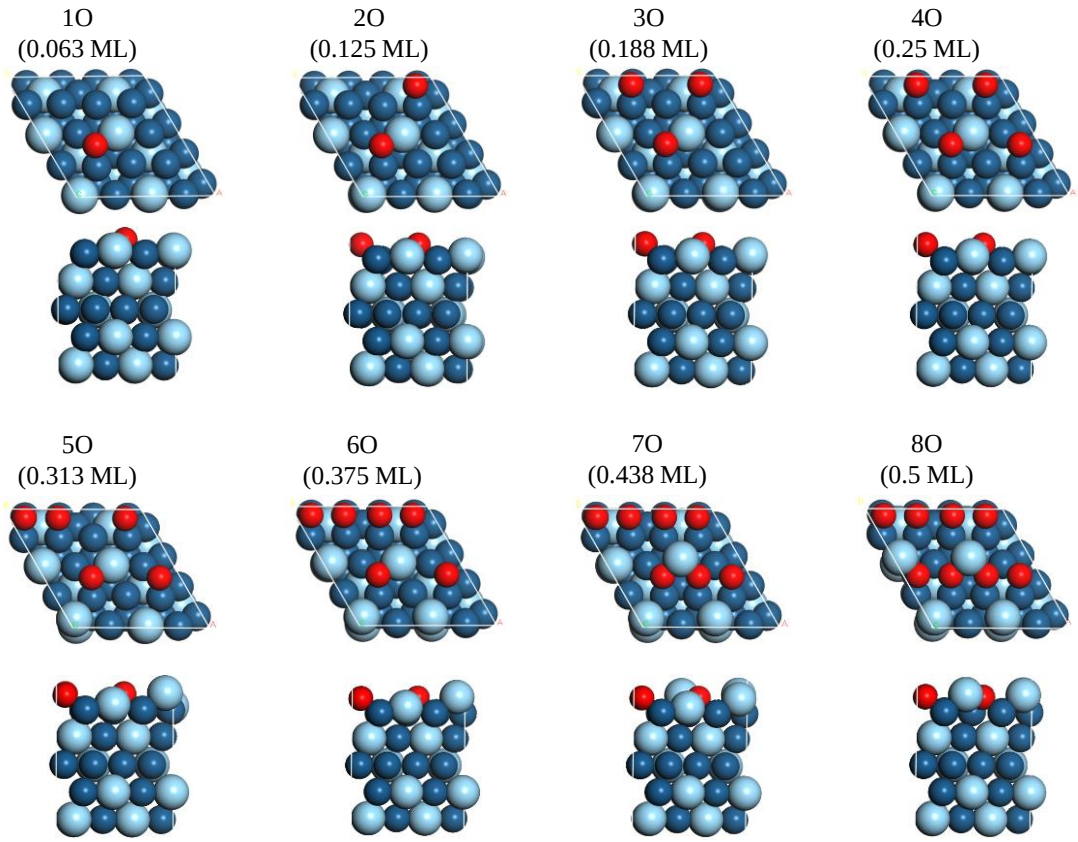

Figure S5. Top and lateral views of the optimized structures for atomic oxygen chemisorbed on Pt_3Sn (111)- $2\sqrt{3}\times4$ for different coverage in ML. Color code for the atomic structures is the same as in Figure S1.

The most stable structures of oxygen adsorption are located in hollow sites containing one tin atom (Pt-Sn-Pt). The corresponding optimized structures for O adsorption on Pt_3Sn (111) at all O coverage are depicted in Figure S5. The calculated Pt-O and Sn-O bond lengths for the lowest oxygen coverage (0.063 ML) are 2.11 and 2.15 Å and the height of O atoms above the Pt_3Sn (111) surface is 1.19 Å. These structures and their corresponding energetics (Figure 2) agree well with the previous work by Dupont et al.[2] Note that the values of Pt-O and Sn-O bond lengths on $Pt_{10}Sn_3O_n/Al_2O_3$ system (Figure S3) for the similar adsorption site (hollow Pt-Sn-Pt) are very similar, 2.13 and 2.21 Å, respectively.

S8. Thermodynamic diagram (P_{O2},T) for the adsorption of atomic O on Pt_{13}/Al_2O_3.

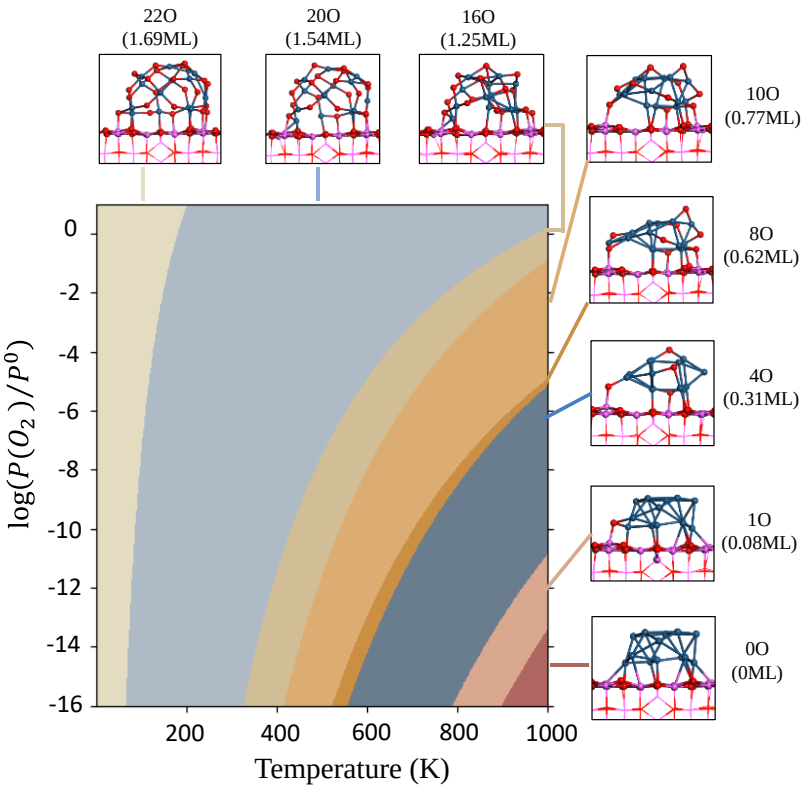

Figure S6. Thermodynamic phase diagram depicting the most stable oxygen coverage as a function of the temperature (K) and the O_2 partial pressure (bar) for Pt_{13}/Al_2O_3 (100) on the obtained structures by Sangnier et al [3]. The structures of the systems exhibiting a significant stability domain are also depicted (side views). Color code for the atomic structures is the same as in Figure S1.

REFERENCES

[1] a) P. Légaré, *Surf. Sci.* **2005**, *580*, 137–144; b) C. Dupont, Y. Jugnet, D. Loffreda, *J. Am. Chem. Soc.* **2006**, *128*, 9129–9136; c) R. F. de Morais, A. A. Franco, P. Sautet, D. Loffreda, *Phys. Chem. Chem. Phys.* **2015**, *17*, 11392–11400;

[2] a) C. Dupont, Y. Jugnet, F. Delbecq, D. Loffreda, *J. Chem. Phys.* **2009**, *130*, 124716; b) R. M. Watwe, R. D. Cortright, M. Mavrikakis, J. K. Nørskov, J. A. Dumesic, *J. Chem. Phys.* **2001**, *114*, 4663–4668;

[3] A. Sangnier, M. Matrat, A. Nicolle, C. Dujardin, C. Chizallet, *J. Phys. Chem. C* **2018**, *122*, 26974–26986.